## REFERENCES AND NOTES

1. R. Majumdar, M. Sixt, C. A. Parent, *Curr. Opin. Cell Biol.* **30**, 33–40 (2014).
2. P. Roca-Cusachs, R. Sunyer, X. Trepat, *Curr. Opin. Cell Biol.* **25**, 543–549 (2013).
3. C.-M. Lo, H.-B. Wang, M. Dembo, Y. L. Wang, *Biophys. J.* **79**, 144–152 (2000).
4. B. C. Isenberg, P. A. Dimilla, M. Walker, S. Kim, J. Y. Wong, *Biophys. J.* **97**, 1313–1322 (2009).
5. M. Raab *et al.*, *J. Cell Biol.* **199**, 669–683 (2012).
6. S. V. Plotnikov, A. M. Pasapera, B. Sabass, C. M. Waterman, *Cell* **151**, 1513–1527 (2012).
7. T. Kawano, S. Kidoaki, *Biomaterials* **32**, 2725–2733 (2011).
8. J. R. Tse, A. J. Engler, *PLOS ONE* **6**, e15978 (2011).
9. L. G. Vincent, Y. S. Choi, B. Alonso-Latorre, J. C. del Álamo, A. J. Engler, *Biotechnol. J.* **8**, 472–484 (2013).
10. L. Bollmann *et al.*, *Front. Cell. Neurosci.* **9**, 363 (2015).
11. L. A. Flanagan, Y.-E. Ju, B. Marg, M. Osterfield, P. A. Janmey, *Neuroreport* **13**, 2411–2415 (2002).
12. F. Liu *et al.*, *J. Cell Biol.* **190**, 693–706 (2010).
13. T. A. Ulrich, E. M. de Juan Pardo, S. Kumar, *Cancer Res.* **69**, 4167–4174 (2009).
14. D. Cai *et al.*, *Cell* **157**, 1146–1159 (2014).
15. E. Donà *et al.*, *Nature* **503**, 285–289 (2013).
16. A. Haeger, K. Wolf, M. M. Zegers, P. Friedl, *Trends Cell Biol.* **25**, 556–566 (2015).
17. A. Bianco *et al.*, *Nature* **448**, 362–365 (2007).
18. B. A. Camley, J. Zimmermann, H. Levine, W.-J. Rappel, *Phys. Rev. Lett.* **116**, 098101 (2016).
19. G. Malet-Engra *et al.*, *Curr. Biol.* **25**, 242–250 (2015).
20. E. Theveneau *et al.*, *Dev. Cell* **19**, 39–53 (2010).
21. R. Sunyer, A. J. Jin, R. Nossal, D. L. Sackett, *PLOS ONE* **7**, e46107 (2012).
22. Materials and methods are available as supplementary materials on *Science* Online.
23. A. Elosegui-Artola *et al.*, *Nat. Mater.* **13**, 631–637 (2014).
24. D. T. Tambe *et al.*, *Nat. Mater.* **10**, 469–475 (2011).
25. E. Bazellières *et al.*, *Nat. Cell Biol.* **17**, 409–420 (2015).
26. C. E. Chan, D. J. Odde, *Science* **322**, 1687–1691 (2008).
27. A. Elosegui-Artola *et al.*, *Nat. Cell Biol.* **18**, 540–548 (2016).
28. J. Escribano, M. T. Sánchez, J. M. García-Aznar, *Comput. Part. Mech.* **1**, 117–130 (2014).
29. A. Berdahl, C. J. Torney, C. C. Ioannou, J. J. Faria, I. D. Couzin, *Science* **339**, 574–576 (2013).
30. P. M. Krafft, R. X. Hawkins, A. S. Pentland, N. D. Goodman, J. B. Tenenbaum, in *Proceedings of the 37th Conference of the Cognitive Science Society* (Cognitive Science Society, 2015).



## ACKNOWLEDGMENTS

The authors acknowledge X. Serra-Picamal, V. Romaric, R. Alert, J. Cadademunt, and all members of the X.T. and P.R.-C. laboratories for stimulating discussions; N. Castro for technical assistance; and G. Charras, G. Scita, and E. Sahai for providing cells. This work was supported by the Spanish Ministry of Economy and Competitiveness (BFU2015-65074-P to X.T., BFU2011-23111 and BFU2014-52586-REDT to P.R.-C., DPI2015-64221-C2-1-R to J.M.G.-A., DPI2013-43727-R to J.J.M., PI14/00280 to D.N., RYC-2014-15559 to V.C., FPI BES-2013-063684 to J.E., IJCI-2014-19156 to A.E.-A., and IJCI-2014-19843 to A.L.), the Generalitat de Catalunya (2014-SGR-927), the European Research Council (CoG-616480 to X.T. and StG 306571 to J.M.G.-A.), Obra Social "La Caixa," Marie-Curie Action (CAFFORCE 328664 to A.L.), EMBO Long-Term Fellowship (EMBO ALTF 1235-2012 to A.L.), a Career Integration Grant within the seventh European Community Framework Programme (PCIG10-GA-2011-303848 to P.R.-C.), and Fundació la Marató de TV3 (project 20133330 to P.R.-C.).


## SUPPLEMENTARY MATERIALS

www.sciencemag.org/content/353/6304/1157/suppl/DC1
Materials and Methods
Supplementary Text
Figs. S1 to S16
Tables S1 and S2
Movies S1 to S10
References (*31*–*43*)

22 March 2016; accepted 27 July 2016
10.1126/science.aaf7119

TUMOR METABOLISM

# Tissue of origin dictates branched-chain amino acid metabolism in mutant *Kras*-driven cancers

**Jared R. Mayers,[1,2]* Margaret E. Torrence,[1,2]* Laura V. Danai,[1] Thales Papagiannakopoulos,[1]† Shawn M. Davidson,[1,2] Matthew R. Bauer,[1] Allison N. Lau,[1] Brian W. Ji,[3] Purushottam D. Dixit,[3] Aaron M. Hosios,[1,2] Alexander Muir,[1] Christopher R. Chin,[1] Elizaveta Freinkman,[1,2,4,5,6] Tyler Jacks,[1,2,6] Brian M. Wolpin,[7] Dennis Vitkup,[3] Matthew G. Vander Heiden[1,2,5,7]‡**

**Tumor genetics guides patient selection for many new therapies, and cell culture studies have demonstrated that specific mutations can promote metabolic phenotypes. However, whether tissue context defines cancer dependence on specific metabolic pathways is unknown. *Kras* activation and *Trp53* deletion in the pancreas or the lung result in pancreatic ductal adenocarinoma (PDAC) or non–small cell lung carcinoma (NSCLC), respectively, but despite the same initiating events, these tumors use branched-chain amino acids (BCAAs) differently. NSCLC tumors incorporate free BCAAs into tissue protein and use BCAAs as a nitrogen source, whereas PDAC tumors have decreased BCAA uptake. These differences are reflected in expression levels of BCAA catabolic enzymes in both mice and humans. Loss of Bcat1 and Bcat2, the enzymes responsible for BCAA use, impairs NSCLC tumor formation, but these enzymes are not required for PDAC tumor formation, arguing that tissue of origin is an important determinant of how cancers satisfy their metabolic requirements.**

The development of new cancer therapeutics relies on underlying genetic features to identify sensitive patients (*1*). Mutations in both *KRAS* and *TP53* are common genetic events found in tumors arising from many tissues, and cancers with these mutations are often difficult to treat (*2*, *3*). These genetic events, as well as others associated with cancer, contribute to the metabolic changes that support biomass accumulation and cancer cell proliferation (*4*). Oncogenic *RAS* signaling increases glucose and glutamine consumption to support anabolic processes including nucleotide, lipid, and nonessential amino acid biosynthesis and can also drive extracellular protein and lipid scavenging (*5*). *TP53* mutations increase glucose consumption and glycolytic flux, whereas inactivation of *TP53* renders cancer cells more dependent on serine uptake and metabolism (*6*).

*KRAS* and *TP53* mutations are found in most human pancreatic tumors (*7*) and are also common in lung adenocarcinoma (*8*). What is known of how mutant *KRAS* or disruption of *TP53* affects cancer metabolism is based on cell culture studies in defined medium, although in vivo nutrient availability varies widely between tissues, and vasculature changes can limit nutrient access within tumors (*9*, *10*). The inability to model these differences in culture has therefore limited understanding of how tissue of origin influences tumor metabolism (*11*). Furthermore, environment can influence metabolic phenotypes in vitro (*12*–*14*), and metabolic dependencies in vivo can differ from those found in vitro (*15*). Metabolic differences between tumor types may also result from cell-autonomous effects, and tumor metabolic gene expression more closely resembles that of its tissue of origin than that of other tumors (*16*). The same oncogenic driver can also cause different metabolic phenotypes in lung and liver tumors (*17*). This raises the possibility that tumor type is a major determinant of some tumor metabolic dependencies in vivo.

Elevated plasma branched-chain amino acid (BCAA) levels are found in early pancreatic ductal adenocarinoma (PDAC) but not in non–small cell lung carcinoma (NSCLC), even when the tumors are initiated by the same genetic events (*18*). To confirm that tumor tissue of origin influences whole-body BCAA metabolism, we used *LSL–Kras*$^{G12D/+}$;*Trp53*$^{flox/flox}$ (KP) mice. We crossed KP mice to mice harboring a *Cre-recombinase* allele driven by a *Pdx-1* promoter (KP$^{-/-}$C model) (*19*) or delivered viral *Cre* to the lungs of these mice (*20*) in order to generate models of PDAC and NSCLC, respectively. Consistent with prior reports (*18*), mice with early PDAC have increased levels of plasma BCAAs, whereas mice with early NSCLC exhibit decreased plasma BCAA levels (fig. S1, A to D). When cells derived from these tumors

[1]Koch Institute for Integrative Cancer Research, Massachusetts Institute of Technology, Cambridge, MA 02139, USA. [2]Department of Biology, Massachusetts Institute of Technology, Cambridge, MA 02139, USA. [3]Center for Computational Biology and Bioinformatics and Department of Systems Biology, Columbia University, New York, NY 10027, USA. [4]Whitehead Institute for Biomedical Research, Nine Cambridge Center, Cambridge, MA 02142, USA. [5]Broad Institute, Seven Cambridge Center, Cambridge, MA 02142, USA. [6]Howard Hughes Medical Institute, Massachusetts Institute of Technology, Cambridge, MA 02139, USA. [7]Dana-Farber Cancer Institute, Boston, MA 02115, USA.
*These authors contributed equally to this work.
†Present address: School of Medicine, New York University, New York, NY 10016, USA. ‡Corresponding author. Email: mvh@mit.edu

are implanted subcutaneously into syngeneic hosts, tumors derived from PDAC cells did not affect plasma BCAA levels (fig. S1E) (*18*), whereas tumors derived from NSCLC cells led to decreased plasma BCAAs (fig. S1F). These results suggest that tumor formation from NSCLC cells can cause depletion of circulating BCAAs.

To trace tissue-specific differences in BCAA metabolism in animals with pancreatic or lung tumors, mice were fed an amino acid–defined diet in which 20% of leucine and valine were $^{13}$C-labeled. All groups of mice exhibited similar levels of plasma $^{13}$C-BCAA enrichment after 1 week of exposure to labeled diets (figs. S2, A and B). Whereas PDAC tumors contained slightly decreased free BCAAs relative to normal pancreas, NSCLC tumors displayed a significant increase in labeled free BCAAs compared with normal lung (Fig. 1A and fig. S2, C and D). These differences are not a reflection of different amino acid compositions of normal or tumor tissue in either the PDAC or NSCLC models (fig. S3). Because BCAAs are essential amino acids that animals cannot synthesize de novo (*21*), these results suggest that unlike PDAC tumors, NSCLC tumors display enhanced BCAA uptake.

BCAAs have several potential metabolic fates in tissues (Fig. 1B). They can be directly incorporated into protein or reversibly transaminated by BCAA transaminase (Bcat) to produce branched-chain α-ketoacids (BCKAs) and glutamate. BCKAs can regenerate BCAAs, be secreted, or be oxidatively decarboxylated by the branched-chain ketoacid dehydrogenase (Bckdh) complex to allow further oxidation of the carbon skeleton (*21*). In agreement with increased BCAA uptake in NSCLC tumors, lung tumors displayed increased labeled BCAA incorporation into protein compared with normal lung, whereas PDAC tumors incorporated less labeled BCAAs relative to normal pancreas (Fig. 1C and fig. S2, E and F). Analysis of metabolites derived from BCAA catabolism revealed that NSCLC tumors also had more labeled α-ketoisocaproate (KIC), the leucine-derived BCKA, whereas no change was observed in levels of this labeled metabolite in PDAC tumors (Fig. 1D and fig. S2G). No other differences in labeled BCAA catabolite levels were observed in NSCLC compared with normal tissues, but PDAC tumors showed decreased labeling of the tricarboxylic acid (TCA) cycle intermediate citrate relative to normal pancreas from labeled BCAAs (Fig. 1E and fig. S2, G to I). This is consistent with recent work demonstrating minimal catabolism of BCAAs to TCA intermediates in proliferating cells (*22*). We then explored whether excess KIC may be excreted by NSCLC tumors for further metabolism by other tissues, such as liver, which has limited Bcat but high Bckdh activity (*21*, *23*). Consistent with this hypothesis, we observed increased labeling of downstream leucine metabolites in the livers of mice with lung tumors (fig. S4). Taken together, these data suggest that BCAA uptake and transamination, but not their subsequent catabolism, may provide a benefit to NSCLC tumors, potentially by acting as a source of nitrogen.

To examine whether NSCLC tumors, but not PDAC tumors, use BCAAs as a source of nitrogen,

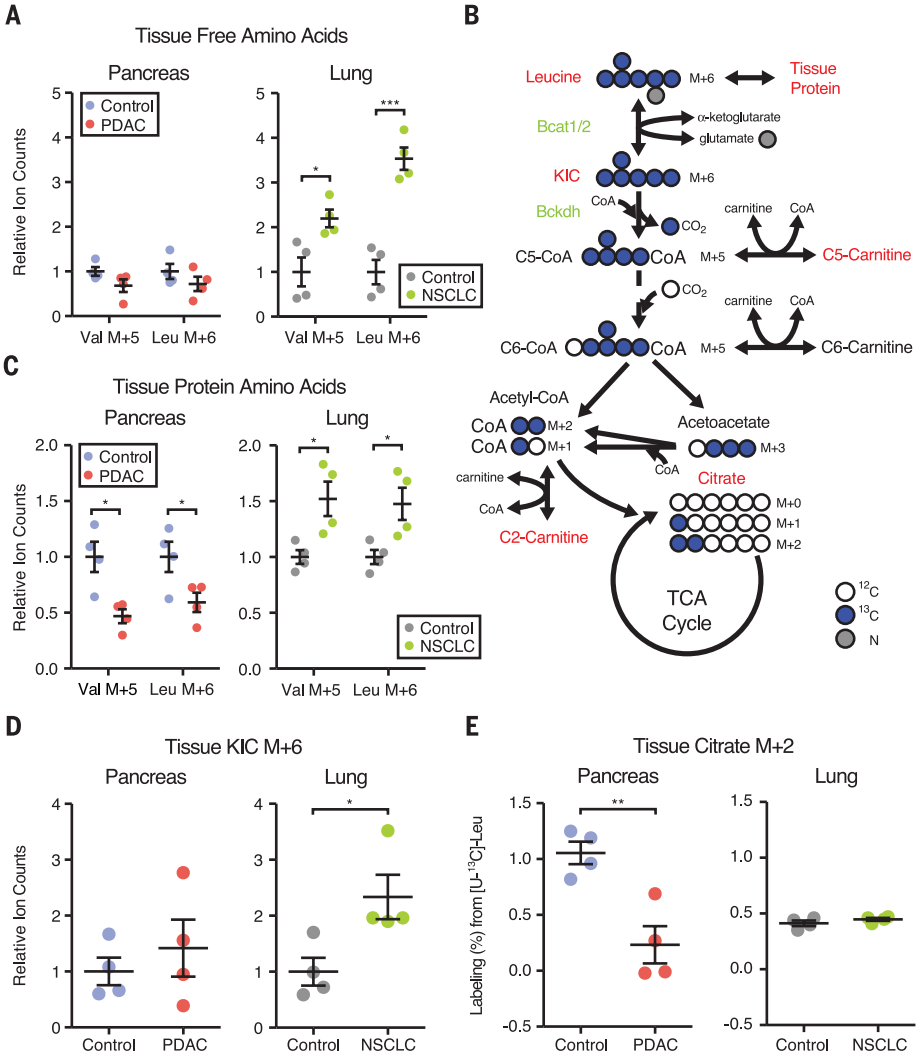


**Fig. 1. Mice with NSCLC display increased BCAA uptake and metabolism.** (**A** and **C** to **E**) Mice were fed $^{13}$C-BCAA–containing diet for 7 days. (A) Relative ion counts by means of liquid chromatography–mass spectrometry (LC-MS) analysis of fully labeled, free BCAAs in tumors from PDAC and NSCLC mice and normal tissues from their respective control mice. Data are presented as mean ± SEM; $n$ = 4 control and $n$ = 4 PDAC; $n$ = 4 control and $n$ = 4 NSCLC. (**B**) Diagram of the leucine catabolic pathway. Red labels indicate metabolites measured with mass spectrometry. Blue circles indicate $^{13}$C-labeled carbons. KIC, α-ketoisocaproate. (C) Relative ion counts by means of gas chromatography (GC)–MS analysis of fully labeled BCAAs from protein acid hydrolysates of tumors from PDAC and NSCLC mice and normal tissues from their respective control mice. Data are presented as mean ± SEM; $n$ = 4 control and $n$ = 4 PDAC; $n$ = 4 control and $n$ = 4 NSCLC. (D) Relative ion counts by means of LC-MS analysis of fully labeled KIC in tumors from PDAC and NSCLC mice and normal tissues from their respective control mice. Data are presented as mean ± SEM; $n$ = 4 control and $n$ = 4 PDAC; $n$ = 4 control and $n$ = 4 NSCLC. (E) Citrate M+2 labeling (%) from [U-$^{13}$C]-leucine by means of GC-MS analysis in tumors from PDAC and NSCLC mice and normal tissues from their respective control mice. Data are presented as mean ± SEM; $n$ = 4 control and $n$ = 4 PDAC; $n$ = 4 control and $n$ = 4 NSCLC. Two-tailed $t$ test was used for all comparisons between two groups. *$P$ < 0.05, **$P$ < 0.01, ***$P$ < 0.001.

we fed mice a modified amino acid diet in which 50% of leucine was labeled with $^{15}$N, allowing the fate of leucine-derived nitrogen to be traced (Fig. 2A). In agreement with $^{13}$C-tracing, mice with PDAC demonstrated no differences in free $^{15}$N-labeled leucine in tumors compared with control pancreas (fig. S5A) and had less $^{15}$N incorporation into other amino acids (fig. S5B). In contrast, increased levels of $^{15}$N-leucine were found in NSCLC tumors compared with normal lung (fig. S5C) with decreased plasma enrichment of $^{15}$N-leucine in mice with NSCLC tumors (Fig. 2B and fig. S5D). A relative increase in $^{15}$N-labeling of nonessential amino acids, as well as valine and isoleucine, was observed in both the free and tissue-protein amino acid pools of NSCLC compared with control lung (Fig. 2C and fig. S5, C and E). Given the reduced plasma enrichment of

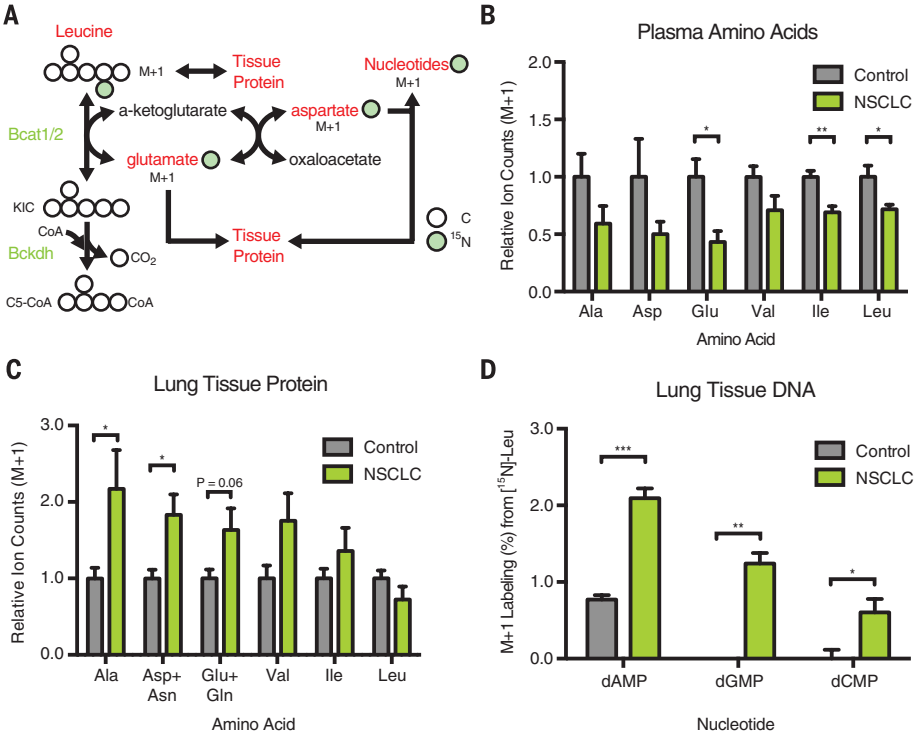


**Fig. 2. BCAA-derived nitrogen supports nonessential amino acid and DNA synthesis in NSCLC tumors.** (**A**) Diagram of leucine transamination by Bcat and nitrogen (green circles) fate after transamination. (**B** to **D**) NSCLC mice were fed $^{15}$N-leucine containing diet for 6 days. (B) Relative ion counts by means of GC-MS analysis of M+1-labeled amino acids in plasma of control and NSCLC mice. Data are presented as mean ± SEM; $n$ = 5 control and $n$ = 6 NSCLC. (C) Relative ion counts by means of GC-MS analysis of M+1-labeled amino acids from protein acid hydrolysates of control mouse lung tissue and NSCLC mouse tumors. Data are presented as mean ± SEM; $n$ = 6 control and $n$ = 6 NSCLC. (D) M+1 labeling (%) from $^{15}$N-leucine of deoxynucleic acids from nucleic acid digest of control mouse lung tissue and NSCLC mouse tumors. Data are presented as mean ± SEM; $n$ = 6 control and $n$ = 6 NSCLC. Two-tailed $t$ test was used for all comparisons between two groups. *$P$ < 0.05, **$P$ < 0.01, ***$P$ < 0.001.

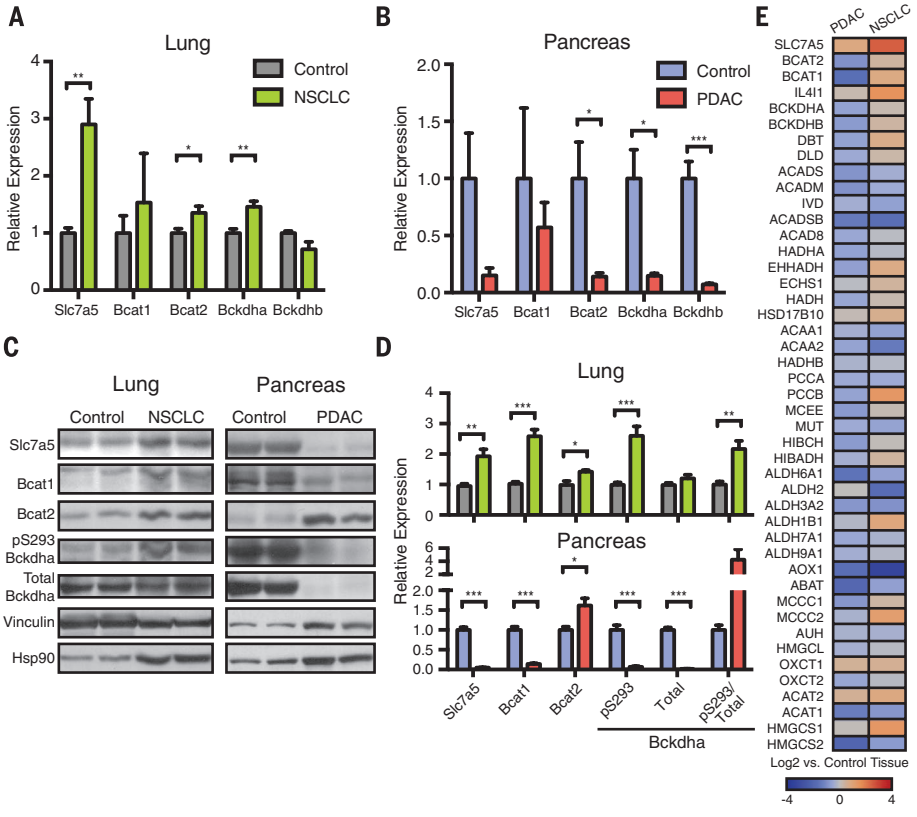


**Fig. 3. Gene expression in both mouse and human tumors reflects tumor tissue–specific BCAA metabolism.** (**A**) Relative expression of BCAA metabolic pathway genes in normal lung and NSCLC tumors from KP mice. Data are presented as mean ± SEM; $n$ = 6 control and $n$ = 6 NSCLC. (**B**) Relative expression of BCAA metabolic pathway genes in normal pancreas and PDAC tumors from KP mice. Data are presented as mean ± SEM; $n$ = 7 control and $n$ = 5 PDAC. (**C**) Immunoblots of proteins involved in BCAA metabolism in representative normal lung and NSCLC tumors (left) and representative normal pancreas and PDAC tumors (right) from KP mice. (**D**) Quantification of (C). Data are presented as mean ± SEM; $n$ = 6 control and $n$ = 6 NSCLC; $n$ = 4 control and $n$ = 4 PDAC. (**E**) Comparison of BCAA metabolic pathway gene expression in human NSCLC and PDAC tumors relative to their adjacent paired normal tissues. Overall expression of BCAA metabolism genes is significantly decreased in PDAC ($P$ < 0.0001). Two-tailed $t$ test was used for all comparisons between two groups unless otherwise stated. *$P$ < 0.05, **$P$ < 0.01, ***$P$ < 0.001.

$^{15}$N-amino acid species (Fig. 2B and fig. S5D), this $^{15}$N-labeling pattern argues that BCAA-transamination mediated by *Bcat* isoforms is active in NSCLC tumor tissue. Evidence for increased BCAA transamination in NSCLC compared with PDAC cells is also evident in vitro across a range of glutamine concentrations; however, tissue culture does not recapitulate the same phenotypes observed in tumors (fig. S6). Downstream of nonessential amino acid biosynthesis, this nitrogen can also be used to generate nucleotides, primarily if aspartate is synthesized de novo in these tumors. Consistent with this possibility, we found increased incorporation of $^{15}$N-label in both aspartate and nucleotides (Fig. 2, C and D, and fig. S5E). In

some contexts, aspartate production is limiting for nucleotide biosynthesis and proliferation (*24*, *25*), indicating that BCAA metabolism may be important for tumor growth.

To test whether gene expression differences might contribute to differential BCAA metabolism, we used quantitative reverse transcription polymerase chain reaction (RT-PCR) to analyze mRNA levels in NSCLC and PDAC tumors compared with their respective normal tissues. Consistent with increased BCAA uptake and KIC generation in NSCLC tumors, these tumors displayed increased expression of the primary BCAA transporter *Slc7a5* (also called the neutral amino acid transporter *Lat1*) and increased levels of *Bcat2* and *Bckdh* (Fig. 3, A, C, and D). In contrast, PDAC exhibited decreased expression of these genes relative to normal pancreas (Fig. 3, B to D). We also observed increased inhibitory phosphorylation of the Bckdh complex in lung tumors (Fig. 3, C and D). *Bcat* expression enables use of BCAAs as a source of nitrogen by lung tumors, and inhibition of Bckdh prevents further catabolism of these amino acids.

The expression changes observed in PDAC are not specific to this model; the related KPC mouse model (*26*), which is initiated by a point mutation in *Trp53*, showed similar changes in gene expression (fig. S7A). Furthermore, these decreases in gene expression do not appear to be a consequence of the relative decrease in cancer cellularity of PDAC tumors (*7*) because sorted pancreatic cancer cells showed similar expression of genes involved in proximal BCAA catabolism relative to whole tumor extracts (fig. S7B). In further agreement with neither lung nor pancreatic cancers showing evidence of downstream BCAA-carbon oxidation, the expression of enzymes from this pathway was not markedly different in either of these cancers (fig. S7, C and D). In contrast, glycolytic gene expression was increased in both tumor types (fig. S7, E and F), which is consistent with known increases in glycolysis in each tumor type (*27*–*29*). Last, to relate these data to tissue of origin, we performed principal component and clustering analyses, which demonstrated segregation of each tumor with the normal tissue from which it arose (figs. S7, G and H).

To ascertain whether similar changes in gene expression were also found in human cancers, we examined expression of BCAA catabolic enzymes in NSCLC and PDAC relative to their respective normal tissues in publicly available data sets (*30*). Consistent with our observations in mice, human NSCLC had increased expression of *SLC7A5*, *BCAT*, and *BCKDH*, whereas expression of BCAA catabolism pathway enzymes was decreased in human PDAC ($P < 0.0001$ for the pathway) (Fig. 3E and tables S1 and S2). The distinct expression patterns for each tumor type were highly correlated across multiple data sets (fig. S7I and tables S3 to S6). The similarity between human NSCLC and the mouse model of NSCLC was observed despite *KRAS* and *TP53* mutations occurring in <50% of human tumors (*8*), and similar expression patterns were also seen in squamous cell lung cancer (fig. S7I and table S6), further supporting the notion that tissue of origin can dictate metabolic phenotype.

The increased contribution of plasma BCAAs to biomass in NSCLC tumors suggests that these tumors may rely on BCAA metabolism for growth. To test this possibility, we used clustered regularly interspaced short palindromic repeats (CRISPR)–Cas9–mediated genome editing to disrupt exon sequences present in both the *Bcat1* (cytosolic) and the *Bcat2* (mitochondrial) isoforms (fig. S8A) in cancer cell lines derived from KP mice with NSCLC (*Bcat* null clones A and B) or PDAC (*Bcat* null) (fig. S8B). Expression analysis and $^{15}$N-leucine tracing studies confirmed functional deletion of

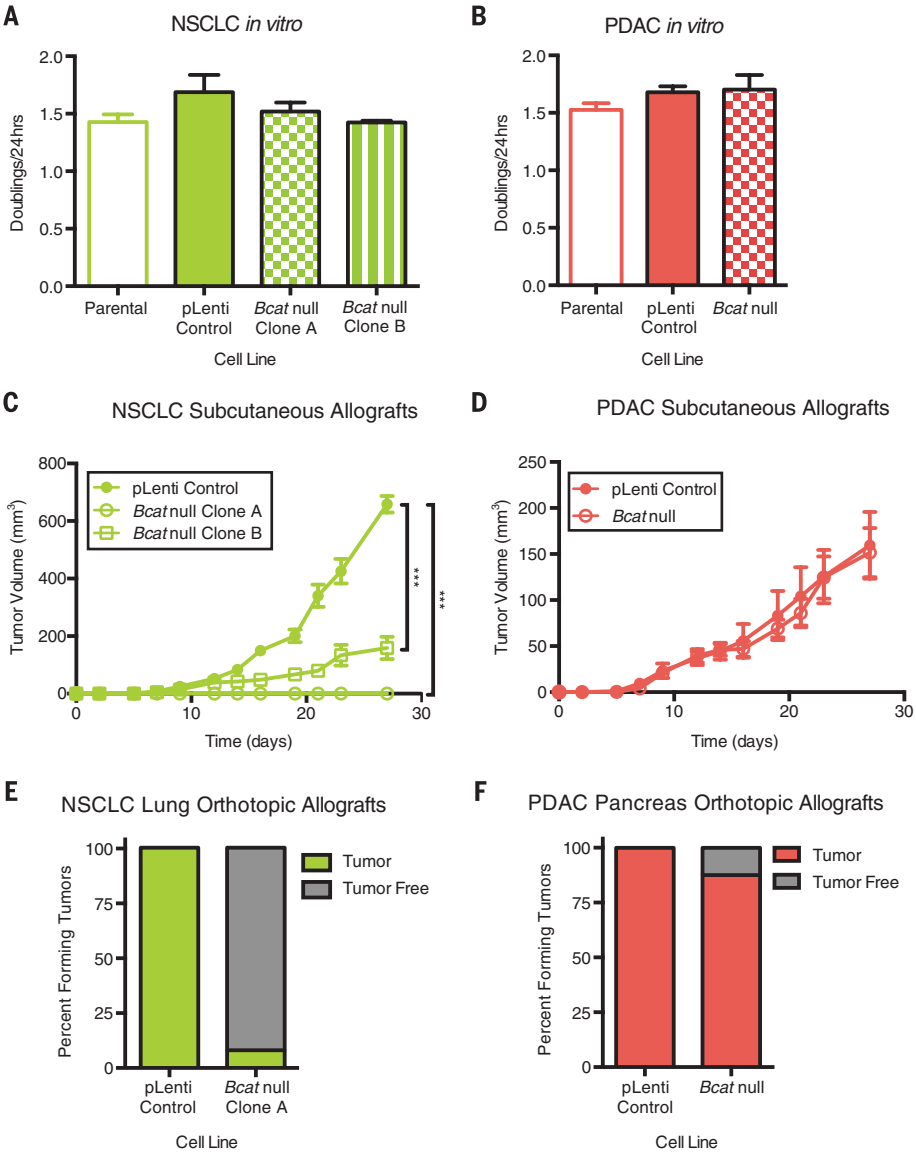


**Fig. 4. Bcat activity is required for NSCLC tumor growth.** (**A**) Doubling time of parental, control CRISPR-Cas9 vector infected (pLenti), and NSCLC *Bcat* null cell lines in vitro. Data are presented as mean ± SEM; $n = 3$ per group. Representative experiment from ≥2 repeats. (**B**) Doubling time of parental, control CRISPR-Cas9 vector infected, and PDAC *Bcat* null cell lines in vitro. Data are presented as mean ± SEM; $n = 3$ per group. Representative experiment from ≥2 repeats. (**C**) Estimated tumor volume (cubic millimeters) of subcutaneous allograft of control infected and *Bcat* null syngenic NSCLC cell lines into C57BL/6J mice. Data are presented as mean ± SEM; $n = 6$ per group. Two-way repeated measures analysis of variance (ANOVA) was used for comparison between groups. (**D**) Estimated tumor volume (cubic millimeters) of subcutaneous allograft of control infected and *Bcat*-null syngenic PDAC cell lines into C57BL/6J mice. Data are presented as mean ± SEM; $n = 5$ pLenti control and $n = 6$ *Bcat* null. Two-way repeated measures ANOVA was used for comparison between groups. (**E**) Lung orthotopic allograft of control infected and *Bcat*-null syngenic NSCLC cell lines into C57BL/6J mice; $n = 23$ vector control and $n = 13$ *Bcat* null Clone A. (**F**) Pancreatic orthotopic allograft of control infected and *Bcat* null syngenic PDAC cell lines into C57BL/6J mice. $n = 8$ mice per group. *$P < 0.05$, **$P < 0.01$, ***$P < 0.001$.

*Bcat* in both the NSCLC and PDAC cancer cells (fig. S8, C to F). Despite loss of both *Bcat* isoforms, these cells proliferate at a rate that is similar to the parental and vector control infected cell lines in vitro (Fig. 4, A and B). When *Bcat*-null NSCLC cells were implanted subcutaneously in vivo, however, the ability of these cells to form tumors was impaired, and one clone failed to produce tumors (Fig. 4C and fig. S8G). In contrast, *Bcat*-null PDAC cells implanted subcutaneously generated tumors (Fig. 4D and fig. S8H). Additionally, orthotopic transplantation of NSCLC *Bcat*-null cells failed to form lung tumors (Fig. 4E), whereas PDAC *Bcat*-null cells formed tumors in the pancreas (Fig. 4F). Unlike subcutaneously implanted PDAC cells in which both *Bcat* isoforms were knocked out, these cells formed smaller tumors in the pancreas than did control cells (fig. S8I). Taken together, these data suggest that although KP lung tumors require Bcat activity for growth, this enzyme activity is dispensable for KP pancreas tumor formation, although PDAC tumor growth may be aided by Bcat activity in some tissue environments.

Proliferating cells need to acquire amino acids, both to make protein and as a source of nitrogen for nucleotide and nonessential amino acid synthesis. Prior work has shown that macropinocytosis plays a role in filling this requirement in mutant *RAS*-driven PDAC tumors and cells (*12*, *14*, *31*). The data presented here argue that this process might be less active in mutant *Ras*–transformed NSCLC tumors that acquire nitrogen in part from free BCAAs. Indeed, we observed less macropinocytosis in cells derived from mouse NSCLC relative to mouse PDAC cells (fig. S9). The decreased reliance of PDAC on free BCAAs, however, does not necessarily imply that uptake of these amino acids would be toxic for this cancer. Overexpressing *Slc7a5* in PDAC cells is sufficient to increase leucine uptake (fig. S10, A and B) but has minimal effects on proliferation in vitro (fig. S10C) or tumor growth in vivo (fig. S10, D and E).

A role for free BCAAs in supplying nitrogen to lung cancers is intriguing in light of recent studies in glioblastoma and NSCLC indicating that glutamine, which is the most abundant plasma amino acid and serves as the major free amino acid substrate for nitrogen and carbon in culture (*32*), contributes less to tumor metabolism in vivo (*33*, *34*). Indeed, glucose-tracing studies in humans and mice demonstrate that glutamine is net synthesized from glucose (*15*, *33*–*37*), and alternative sources of nitrogen are required to support glutamine production. Thus, in these contexts, extraction of nitrogen from BCAAs for de novo amino acid and nucleotide biosynthesis in vivo may explain how lung tumors satisfy their nitrogen requirements. Consistent with this possibility, *BCAT1* expression is known to be important for glioblastoma growth (*38*), suggesting that tumors arising in tissues other than the lung may also use BCAAs as a source of nitrogen. Multiple factors—including local environment, tumor cell of origin, and genetic mutations—can lead to convergent metabolic adaptations in disparate tumor types.

Elevations in plasma BCAA levels are associated with early PDAC and result from increased tissue protein breakdown (*18*). The finding that PDAC tumors have decreased use of circulating BCAAs contributes to this phenotype as well. In contrast, NSCLC tumors actively use BCAAs, leading to plasma BCAA depletions, particularly because the liver does not regulate levels of these amino acids (*23*). Many patients with PDAC and NSCLC tumors develop cachexia with end-stage disease (*39*). Our findings suggest that differential use of amino acids by tumors and the resulting impact on whole-body metabolism might play a role in the initiation and natural history of cachexia. In addition, as personalized medicine plays a larger role in the clinical management of cancer, it will be critical to understand how cell of origin and tissue environment interact with genetic events to influence metabolic dependencies of tumors and select the right treatment approaches for patients.

## REFERENCES AND NOTES


1. L. A. Garraway, *J. Clin. Oncol.* **31**, 1806–1814 (2013).
2. N. Vasan, J. L. Boyer, R. S. Herbst, *Clin. Cancer Res.* **20**, 3921–3930 (2014).
3. P. A. Muller, K. H. Vousden, *Cancer Cell* **25**, 304–317 (2014).
4. L. K. Boroughs, R. J. DeBerardinis, *Nat. Cell Biol.* **17**, 351–359 (2015).
5. E. White, *Development* **27**, 2065–2071 (2013).
6. F. Kruiswijk, C. F. Labuschagne, K. H. Vousden, *Nat. Rev. Mol. Cell Biol.* **16**, 393–405 (2015).
7. A. V. Biankin *et al.*, *Nature* **491**, 399–405 (2012).
8. E. A. Collisson *et al.*, *Nature* **511**, 543–550 (2014).
9. P. Vaupel, F. Kallinowski, P. Okunieff, *Cancer Res.* **49**, 6449–6465 (1989).
10. A. Hirayama *et al.*, *Cancer Res.* **69**, 4918–4925 (2009).
11. J. R. Mayers, M. G. Vander Heiden, *Trends Biochem. Sci.* **40**, 130–140 (2015).
12. C. Commisso *et al.*, *Nature* **497**, 633–637 (2013).
13. J. J. Kamphorst *et al.*, *Proc. Natl. Acad. Sci. U.S.A.* **110**, 8882–8887 (2013).
14. W. Palm *et al.*, *Cell* **162**, 259–270 (2015).
15. S. M. Davidson *et al.*, *Cell Metab.* **23**, 517–528 (2016).
16. J. Hu *et al.*, *Nat. Biotechnol.* **31**, 522–529 (2013).
17. M. O. Yuneva *et al.*, *Cell Metab.* **15**, 157–170 (2012).
18. J. R. Mayers *et al.*, *Nat. Med.* **20**, 1193–1198 (2014).
19. N. Bardeesy *et al.*, *Proc. Natl. Acad. Sci. U.S.A.* **103**, 5947–5952 (2006).
20. M. DuPage, A. L. Dooley, T. Jacks, *Nat. Protoc.* **4**, 1064–1072 (2009).
21. A. E. Harper, R. H. Miller, K. P. Block, *Annu. Rev. Nutr.* **4**, 409–454 (1984).
22. C. R. Green *et al.*, *Nat. Chem. Biol.* **12**, 15–21 (2016).
23. J. T. Brosnan, *J. Nutr.* **133** (suppl. 1), 2068S–2072S (2003).
24. K. Birsoy *et al.*, *Cell* **162**, 540–551 (2015).
25. L. B. Sullivan *et al.*, *Cell* **162**, 552–563 (2015).
26. S. R. Hingorani *et al.*, *Cancer Cell* **7**, 469–483 (2005).
27. H. Friess *et al.*, *Gut* **36**, 771–777 (1995).
28. K. Kubota *et al.*, *J. Nucl. Med.* **31**, 1927–1932 (1990).
29. K. B. Nolop *et al.*, *Cancer* **60**, 2682–2689 (1987).
30. T. Barrett *et al.*, *Nucleic Acids Res.* **39** (database), D1005–D1010 (2011).
31. J. J. Kamphorst *et al.*, *Cancer Res.* **75**, 544–553 (2015).
32. R. J. DeBerardinis *et al.*, *Proc. Natl. Acad. Sci. U.S.A.* **104**, 19345–19350 (2007).
33. I. Marin-Valencia *et al.*, *Cell Metab.* **15**, 827–837 (2012).
34. K. Sellers *et al.*, *J. Clin. Invest.* **125**, 687–698 (2015).
35. E. A. Maher *et al.*, *NMR Biomed.* **25**, 1234–1244 (2012).
36. S. Tardito *et al.*, *Nat. Cell Biol.* **17**, 1556–1568 (2015).
37. C. T. Hensley *et al.*, *Cell* **164**, 681–694 (2016).
38. M. Tönjes *et al.*, *Nat. Med.* **19**, 901–908 (2013).
39. W. D. Dewys *et al.*, *Am. J. Med.* **69**, 491–497 (1980).


## ACKNOWLEDGMENTS


J.R.M. acknowledges support from U.S. NIH National Cancer Institute (NCI) grant F30CA183474 and National Institute of General Medical Sciences grant T32GM007753. A.N.L. is a Robert Black Fellow of the Damon Runyon Cancer Research Foundation, DRG-2241-15. M.G.V.H. acknowledges support from NCI grants P30CA1405141, R01CA168653, and R01CA201276; the Burroughs Wellcome Fund; the Eisen and Chang Families; the Ludwig Center at Massachusetts Institute of Technology; Stand Up To Cancer; and the Lustgarten Foundation. M.G.V.H. is a paid scientific adviser for Agios Pharmaceuticals and for Aeglea Biotherapeutics, biotechnology companies that are developing drugs targeting cellular metabolism to treat cancer and other diseases.


## SUPPLEMENTARY MATERIALS

www.sciencemag.org/content/353/6304/1161/suppl/DC1
Materials and Methods
Figs. S1 to S10
Tables S1 to S8
References (*40*–*49*)


21 February 2016; accepted 29 July 2016
10.1126/science.aaf5171

**Tissue of origin dictates branched-chain amino acid metabolism in mutant *Kras*-driven cancers**

Jared R. Mayers, Margaret E. Torrence, Laura V. Danai, Thales Papagiannakopoulos, Shawn M. Davidson, Matthew R. Bauer, Allison N. Lau, Brian W. Ji, Purushottam D. Dixit, Aaron M. Hosios, Alexander Muir, Christopher R. Chin, Elizaveta Freinkman, Tyler Jacks, Brian M. Wolpin, Dennis Vitkup and Matthew G. Vander Heiden (September 8, 2016)

*Science* **353** (6304), 1161-1165. [doi: 10.1126/science.aaf5171]

Editor's Summary



*Science* (print ISSN 0036-8075; online ISSN 1095-9203) is published weekly, except the last week in December, by the American Association for the Advancement of Science, 1200 New York Avenue NW, Washington, DC 20005. 